

## ORIGINAL ARTICLE

# Curcumin induces ferroptosis in non-small-cell lung cancer via activating autophagy

Xin Tang<sup>†</sup>  | Hui Ding<sup>†</sup> | Maoli Liang<sup>†</sup>  | Xing Chen | Yuxia Yan |  
Nansheng Wan | Qianqian Chen  | Jing Zhang | Jie Cao 

Department of Respiratory and Critical Care Medicine, Tianjin Medical University General Hospital, Tianjin, China

**Correspondence**

Jie Cao, Department of Respiratory and Critical Care Medicine, Tianjin Medical University General Hospital, 154 Anshan Road, Heping District, Tianjin 300052, China.  
Email: tjcaojie@163.com

**Funding information**

National key research and development program of China, Grant/Award Number: 2016YFC1304502; National Natural Science Foundation of China, Grant/Award Numbers: 81670084, 81970084; Tianjin Key Research and Development Program, Grant/Award Number: 20YFZCSY00390

**Abstract**

**Background:** Emerging studies showed curcumin can inhibit glioblastoma and breast cancer cells via regulating ferroptosis. However, the role of ferroptosis in the inhibitory effect of curcumin on non-small-cell lung cancer (NSCLC) remains unclear.

**Methods:** Cell counting kit-8 (CCK-8) assay was used to measure the viability of A549 and H1299 cells under different conditions. Cell proliferation was examined by Ki67 immunofluorescence. The morphological changes of cells and tumor tissues were observed by optical microscope and hematoxylin and eosin (H&E) staining. Intracellular reactive oxygen species (ROS), malondialdehyde (MDA), superoxide dismutase (SOD), glutathione (GSH), and iron contents were determined by corresponding assay kit. The related protein expression levels were detected by western blot and immunohistochemistry. Transmission electron microscope was used to observe ultrastructure changes of A549 and H1299 cells.

**Results:** Curcumin inhibited tumor growth and cell proliferation, but promoted cell death. Characteristic changes of ferroptosis were observed in curcumin group, including iron overload, GSH depletion and lipid peroxidation. Meanwhile, the protein level of ACSL4 was higher and the levels of SLC7A11 and GPX4 were lower in curcumin group than that in control group. Incubation of ferroptosis inhibitors ferrostatin-1 (Fer-1) or knockdown of iron-responsive element-binding protein 2 (IREB2) notably weakened curcumin-induced anti-tumor effect and ferroptosis in A549 and H1299 cells. Further investigation suggested that curcumin induced mitochondrial membrane rupture and mitochondrial cristae decrease, increased autolysosome, increased the level of Beclin1 and LC3, and decreased the level of P62. Curcumin-induced autophagy and subsequent ferroptosis were both alleviated with autophagy inhibitor chloroquine (CQ) or siBeclin1.

**Conclusion:** Curcumin induced ferroptosis via activating autophagy in NSCLC, which enhanced the therapeutic effect of NSCLC.

**KEYWORDS**

Autophagy, curcumin, ferroptosis, non-small-cell lung cancer

## INTRODUCTION

Previous data have indicated that lung cancer continues to be one of the commonest malignant tumors and the world's leading cause of cancer death.<sup>1</sup> Non-small-cell lung

cancer (NSCLC) accounts for ~85% of lung cancer.<sup>2</sup> It has made remarkable progress both in traditional treatment and the emerging approaches like molecular targeted therapy, anti-angiogenesis therapy, and immunotherapy,<sup>3,4</sup> although morbidity and mortality of NSCLC remain particularly high. Therefore, a novel anti-tumor method is urgently needed.

<sup>†</sup>Xin Tang, Hui Ding and Maoli Liang contributed equally to this work

Ferroptosis is a newly discovered regulatory cell death (RCD),<sup>5</sup> which is different from other forms of RCD. The accumulation of intracellular iron and lipid-reactive oxygen species (ROS), lipid peroxidation, and the depletion of glutathione (GSH) are the indispensable hallmarks of ferroptosis.<sup>6</sup> Emerging studies have shown that ferroptosis pathway can repress tumor growth and kill tumor cells,<sup>7</sup> which may be a new idea for antitumor treatment. Therefore, ferroptosis inducers are expected to provide potential strategies for anticancer treatment, which has attracted wide attention.

Curcumin is a yellow polyphenol compound derived from the turmeric plant, which shows anticancer properties through a variety of mechanisms, including inhibition of tumor proliferation, invasion and metastases, regulation of apoptosis, and autophagy.<sup>8</sup> Recent studies showed that curcumin can treat glioblastoma and breast cancer via regulating ferroptosis.<sup>9,10</sup> However, there seem to be few studies exploring the relationship of ferroptosis and anti-NSCLC induced by curcumin. Therefore, it is crucial to understand the specific role and potential mechanism of ferroptosis in the anti-NSCLC treatment of curcumin. Previous studies have demonstrated that autophagy promotes ferroptosis.<sup>11</sup> Nevertheless, the specific role of autophagy in curcumin-induced ferroptosis in NSCLC remains unclear.

In this study, we have investigated whether ferroptosis was beneficial to the anti-NSCLC effect of curcumin. Furthermore, we have explored whether the activation of the autophagy pathway promoted ferroptosis in NSCLC.

## MATERIAL AND METHODS

### Reagents

Curcumin (Cur, C7727), chloroquine (CQ, C6628) and ferrostatin-1 (Fer-1, SML0583) were obtained from Sigma Aldrich. Cell counting kit-8 assay (CCK-8, C6005) was purchased from United States (US) Everbright. ROS (E004-1-1), malondialdehyde (MDA, A003-1), and superoxide dismutase (SOD, A001-3) detection kit were obtained from Nanjing Jiancheng Bioengineering Institute. Glutathione (GSH) Assay Kit (S0053) was purchased from Beyotime Biotechnology. ACSL4 (sc-271 800) was purchased from Santa Cruz Biotechnology. SLC7A11 (A2413), IREB2(A6382), and  $\beta$ -actin (AC004) were obtained from ABclonal. GPX4 (ab125066) was purchased from Abcam. Beclin1 (3495), LC3 (12741S), P62 (39749), and Ki67 (12075) were purchased from Cell Signaling Technology (CST).

### Lewis lung carcinoma mice model

Female C57BL/6 mice (14–18 g) were purchased from SiPeiFu (Beijing) Biotechnology. All experimental procedures were accomplished complying with the guidelines for the Care and Use of Laboratory Animals of Tianjin Medical University(Tianjin, China). The protocol was approved by the Animal Ethical and Welfare Committee(AEWC) of Tianjin

Medical University. C57BL/6 mice were subcutaneously injected with a total of  $6 \times 10^5$  Lewis lung carcinomas (LLC) cells on the left flank. Four days after LLC inoculation, the mice were randomly divided into two groups of five. The vehicle control and curcumin groups were given sodium carboxymethyl cellulose (CMC) or curcumin (100 mg/kg/day) by intraperitoneal injection for 15 days. Tumor volume was measured with a caliper every 3 days to track tumor growth and calculated with the following formula:  $0.5 \times \text{length} \times \text{width}$ .<sup>2</sup> Mice were weighed every 3 days to assess the toxicity of the drug. The mice were sacrificed under deep anesthesia, and tumor tissue was removed.

### Histological analysis

Tumor tissues collected from LLC-bearing mice were fixed in 10% neutral buffered formalin and embedded in paraffin. Tumor tissues were then cut to 4- $\mu\text{m}$  thickness, and the sections were dewaxed. The sections were then stained with hematoxylin and eosin (H&E) (Beyotime, Shanghai, China). Stained sections were used to observe the structure of tumor tissue and cell morphology under a light microscope.

### Cell proliferation assay in tumor tissue

The expression of Ki67 was used to detect cell proliferation. After dewaxing, the antigen was recovered with citrate buffer (Sangon Biotech, Shanghai, China) in high temperature and high pressure conditions. Tumor sections were then blocked with 5% normal goat serum (NGS) for 1 hour at room temperature and then incubated with the antibody against Ki67 overnight at 4°C. Subsequently, sections were washed in phosphate buffer saline (PBS) and treated with Cy3-conjugated anti-rabbit IgG (1: 400; Beyotime, A0516). Fluorescent images were obtained on a photomicroscope (Leica DM5000B, Germany).

### Immunohistochemical staining

After the antigen was recovered, the sections were incubated with 3%  $\text{H}_2\text{O}_2$  for 10 minutes, then blocked in 5% NGS at room temperature for 1 hour. Subsequently, the sections were incubated with primary antibodies for ACSL4 and GPX4 overnight at 4°C and anti-mouse/rabbit for 15 minutes. After that, an HRP-DAB system (Beyotime, Shanghai, China) was applied to detect the immunoactivity. The sections were imaged under a light microscope. Images were quantified by Image-Pro Plus 6.0 analysis software.

### Cell culture

The human lung cancer cell line, A549, and H1299 cells were cultured in RPMI-1640 medium containing 10% fetal bovine serum. The cells were incubated under humidified conditions at 37°C and 5%  $\text{CO}_2$ .

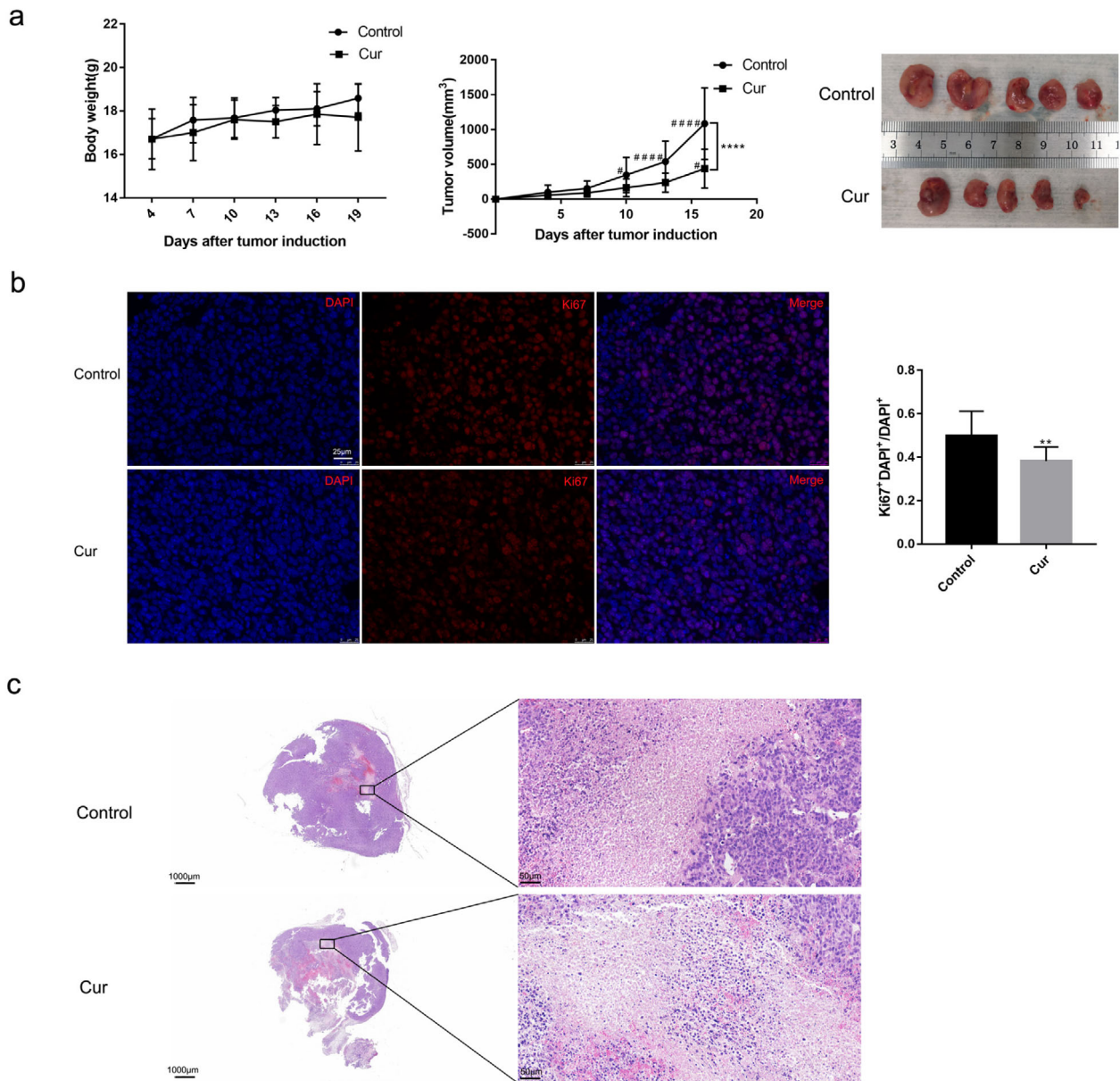


**FIGURE 1** Curcumin inhibits tumor growth and promotes tumor cells death in mice. LLC-bearing female C57BL/6 mice were subjected to curcumin (100 mg/kg/day) by intraperitoneal injection for 15 day ( $n = 5$ ). (a) Body weight of mice, tumor volume, and image of tumors in mice after curcumin treatment. (b) Ki67 immunofluorescence was conducted to detect the proliferation of lung cancer cells (scale bar = 25  $\mu\text{m}$ ). (c) H&E staining of tumor tissue sections was analyzed (left: scale bar = 1000  $\mu\text{m}$ , right: scale bar = 50  $\mu\text{m}$ ). All results are expressed as the mean  $\pm$  SD.  $**P < 0.002$ ,  $****P < 0.0001$  versus control group.  $^{\#}P < 0.05$ ,  $####P < 0.0001$  versus day 4

## Transfections

The A549 and H1299 cells were transfected with 50 nM of IREB2 siRNA, Beclin1 siRNA, and control siRNA (RIBOBIO, Guangzhou, China), respectively, using riboFECTCP transfection kit (RIBOBIO, Guangzhou, China). The target sequence of IREB2 siRNA was “GGCTCATCAAATAAACTTA,” and the target sequence of Beclin1 siRNA was “GGAGTCTCTGACAGACAAA”. We diluted 5  $\mu\text{L}$  of 20  $\mu\text{M}$  siRNAs with 120  $\mu\text{L}$  riboFECTCP buffer, then added 12  $\mu\text{L}$  of riboFECTCP reagent, mixed it gently, and incubated it at room temperature for 5 min. The transfection mixture was then transferred into

6-well plates combined with 1863  $\mu\text{L}$  of RPMI1640 media without penicillin–streptomycin. After 2 hours, A549 and H1299 cells were incubated with curcumin for another 24 hours and subjected to western blot analysis.

## Transmission electron microscope assay

A549 and H1299 cells were cultured under different conditions before being trypsinized and fixed in 2.5% glutaraldehyde. Subsequently, cells were post-fixed in 1% osmium tetroxide with 0.1% potassium ferricyanide, dehydrated through a graded

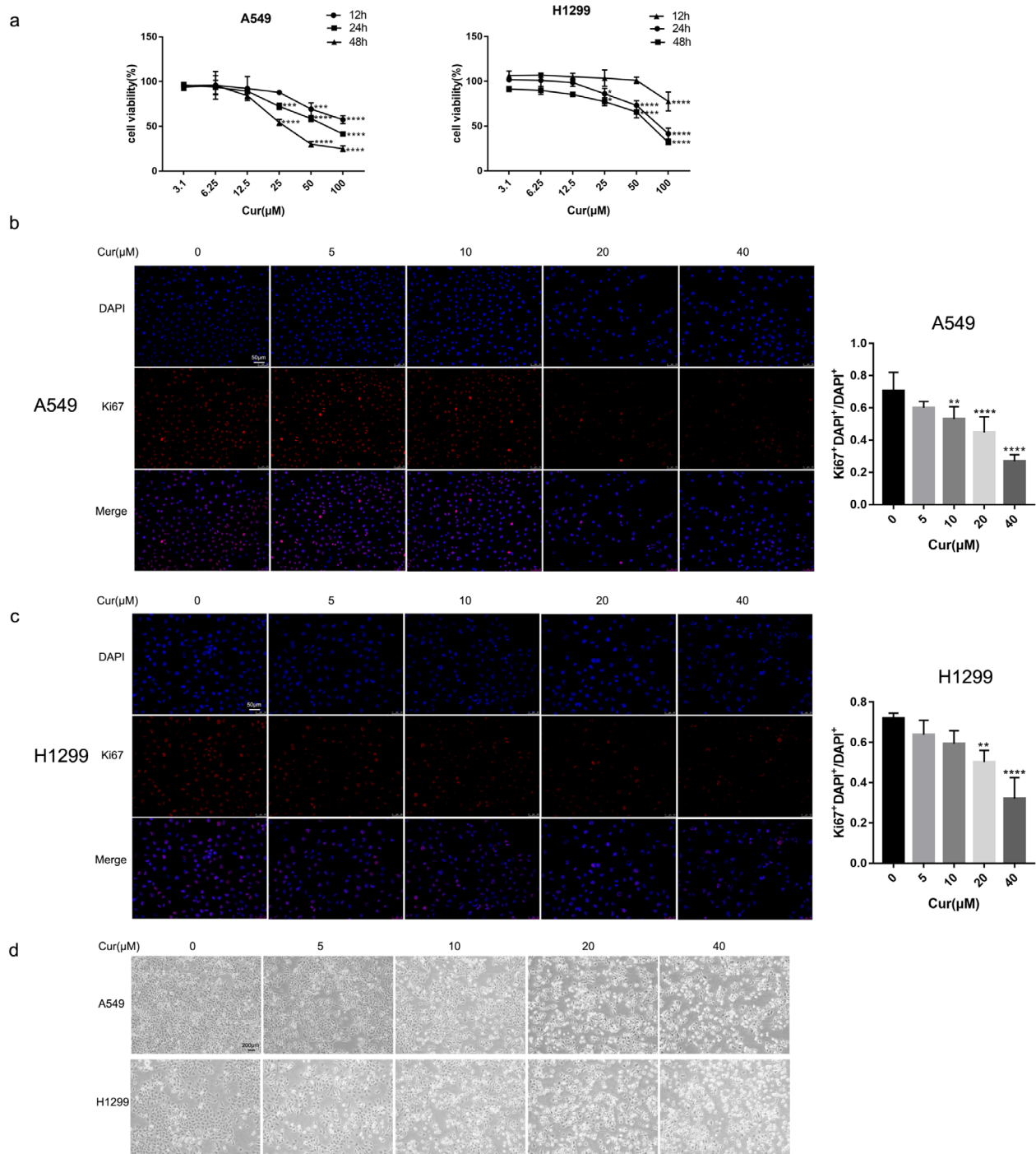


**FIGURE 2** Curcumin inhibits cell proliferation and triggers cell death in A549 and H1299 cells. The cells were treated with curcumin at different concentrations. **(a)** The viability of A549 and H1299 cells with various curcumin concentrations for different time. **(b), (c)** The proliferation of A549 and H1299 cells was detected by Ki67 staining (scale bar = 50 μm). **(d)** Representative cell morphological changes are shown (scale bar = 200 μm). All experiments were done more than three times independently, and all results are expressed as the mean ± SD. \* $P < 0.05$ , \*\* $P < 0.002$ , \*\*\* $P < 0.0002$ , \*\*\*\* $P < 0.0001$  versus control group

series of ethanol (50%–100%), and embedded in epoxy resin. Samples were cut into ultrathin sections (60–80 nm) using an ultramicrotome (Leica EM UC7, Solms, Germany). Ultrathin sections were stained with 2% uranyl acetate saturated alcohol solution and lead citrate, and the images were acquired using a HITACHI-HT7700 transmission electron microscope (Tokyo, Japan; magnification  $\times 7000$ ).

### Measurement of cell viability

A CCK-8 assay kit was used to examine the cell viability. Transfected or non-transfected A549 and H1299 cells were suspended in RPMI-1640 medium and seeded into 96-well culture plates with a density of 5000 cells per well for 12 hours. Cells were then

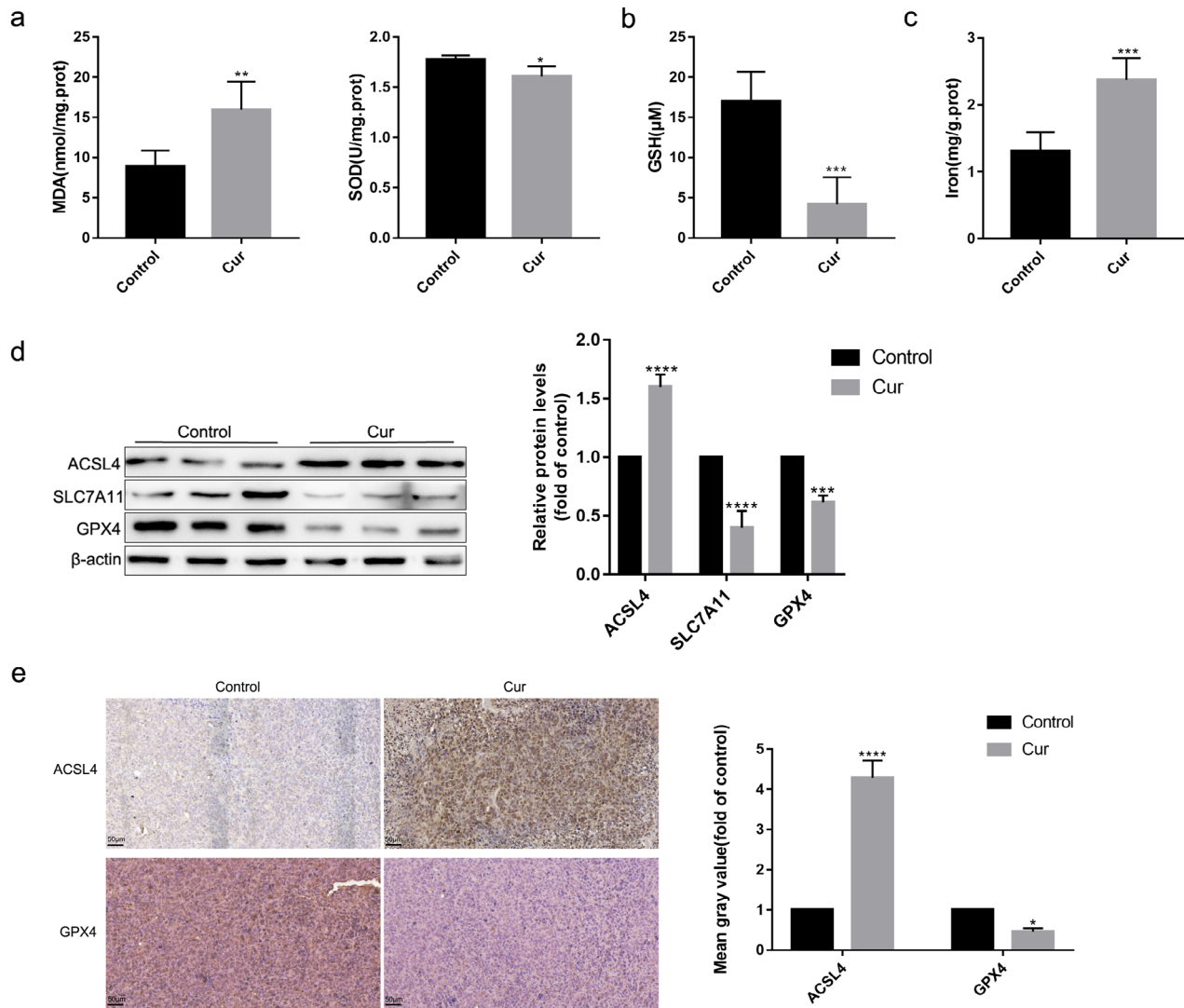


**FIGURE 3** The ferroptosis-related changes induced by curcumin in the tumor tissues of LLC-bearing mice. (a)–(c) Contents of MDA, SOD, GSH, and iron in tumor tissue of mice. (d) Protein levels of ACSL4, SLC7A11, and GPX4 in tumor tissue lysates. (e) Immunohistochemical staining results and semi-quantification analyses of ACSL4 and GPX4 in tumor tissues. All experiments were done more than three times independently, and all results are expressed as the mean  $\pm$  SD. \* $P < 0.05$ , \*\* $P < 0.002$ , \*\*\* $P < 0.0002$ , \*\*\*\* $P < 0.0001$  versus control group

cultured with different concentrations of curcumin, Fer-1, and CQ. CCK-8 solution was added after that at 10  $\mu$ L/well, and cells were incubated for an additional 2 hours. The absorbance at 450 nm measured by a microplate reader (BioTek, Winooski, VT) was applied to analyze the cell viability.

### Cell proliferation assay in A549 and H1299 cells

The A549 and H1299 cells were incubated with 30  $\mu$ M of curcumin after being seeded on glass coverslips for 24 hours. The slides were fixed in 4% paraformaldehyde and permeabilized in 0.2% Triton X-100. The coverslips were blocked with 5% NGS for 1 hour at room temperature and then stayed overnight at 4°C with the antibody against Ki67 (1:200). Subsequently, the coverslips were incubated with

Cy3-conjugated anti-rabbit IgG. Fluorescent images were obtained on a photomicroscope.

### Determination of ROS, MDA, SOD, and GSH levels

In accordance with the manufacturer's instructions, the intracellular ROS was measured using peroxide-sensitive fluorescent probe DCFH-DA. Briefly, A549 and H1299 cells were incubated with 10  $\mu$ M of DCFH-DA at 37°C for 1 hour, and the fluorescence intensity was calculated with flow cytometry.

On the basis of the manufacturer's instructions, the contents of MDA and the activity of SOD were measured by relevant reagent kits. First, A549 and H1299 cells were harvested and ultrasonicated, and the tumor tissue was homogenized. Second,

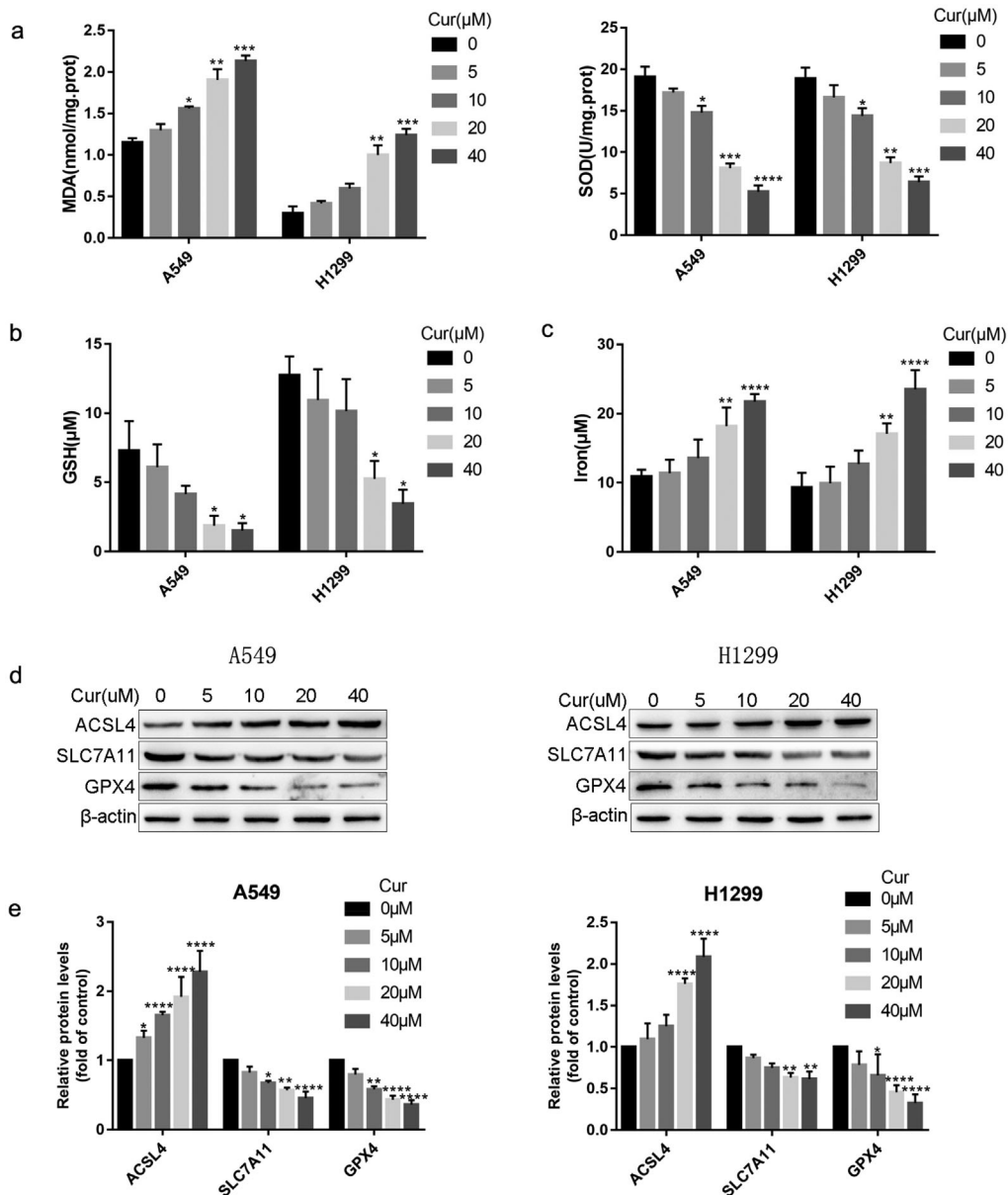


**FIGURE 4** Curcumin triggers ferroptosis-related changes in A549 and H1299 cells. (a)–(c) The MDA, SOD, GSH, and iron contents in A549 and H1299 cells were measured using corresponding kits. (d) The protein levels of ACSL4, SLC7A11, and GPX4 were examined by western blotting. All experiments were done more than three times independently, and all results are expressed as the mean  $\pm$  SD. \* $P < 0.05$ , \*\* $P < 0.002$ , \*\*\* $P < 0.0002$ , \*\*\*\* $P < 0.0001$  versus control group

according to the protein concentration of cells and tissues, MDA contents and SOD activity were evaluated and normalized.

The total quantity of glutathione was examined by GSH and GSSG assay kit and performed in accordance with the manufacturer's instructions. The contents of GSH were evaluated by comparing with the standard curve of GSH.

### Iron assay

The contents of iron in A549 and H1299 cells were determined according to the manufacturer's instructions (E1042, Beijing Applygen Technologies, China). The iron content of

tumor tissue was measured by tissue iron assay kit (A039-2, Nanjing Jincheng Bioengineering Institute, China).

### Western blot

Total proteins were extracted from cells and tumor tissue. The BCA assay kit (Thermo Fisher Scientific, Shanghai, China) was used to evaluate protein concentration. Sodium dodecyl sulfate-polyacrylamide gel electrophoresis (SDS-PAGE) was applied to separate proteins. The proteins were transferred to polyvinylidene fluoride (PVDF) membranes. Subsequently, membranes were incubated with primary antibodies at 4°C overnight

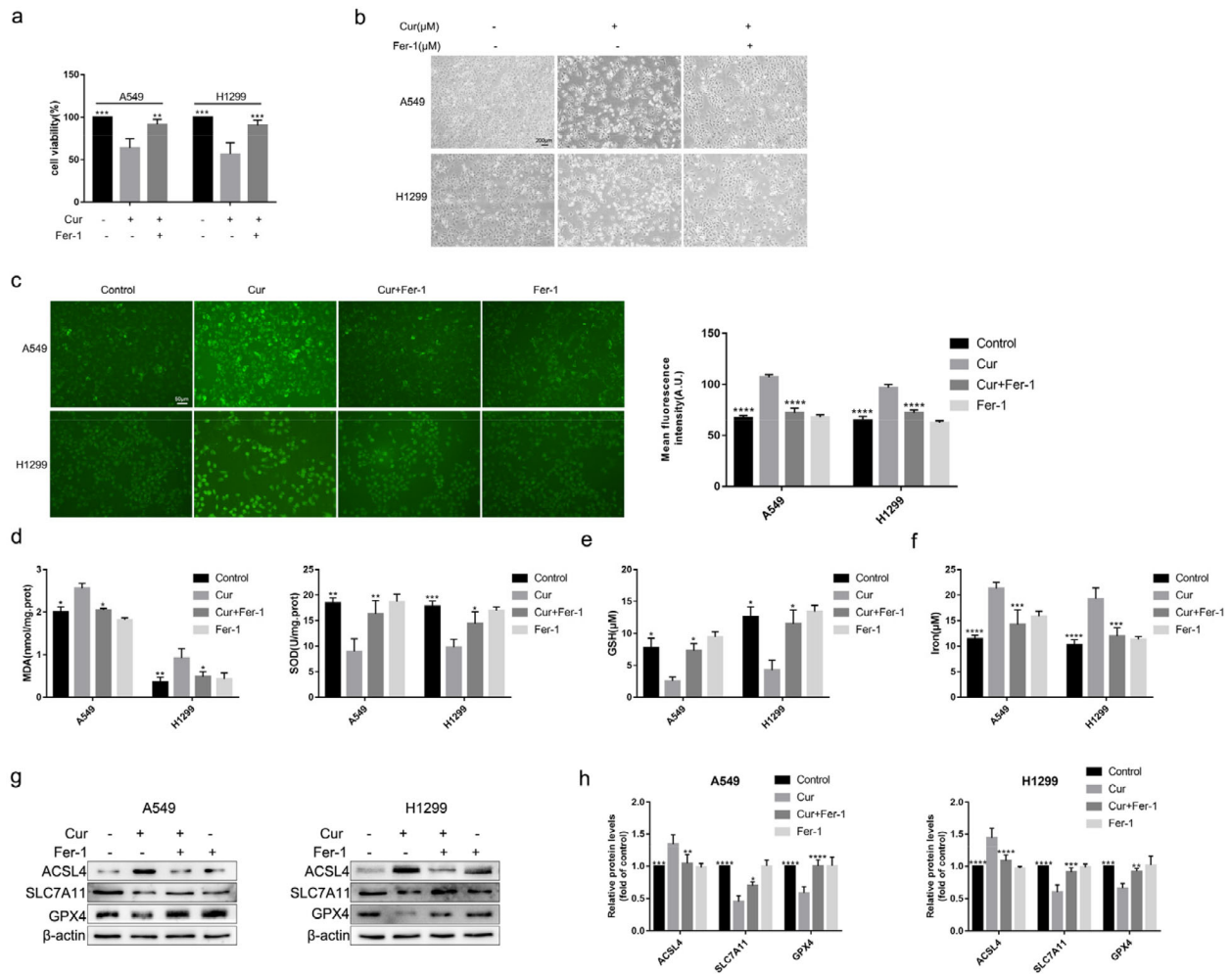


**FIGURE 5** Inhibition of ferroptosis by Fer-1 attenuates cell death induced by curcumin in A549 and H1299 cells. (a) The viability of A549 and H1299 cells with 30  $\mu\text{mol/L}$  curcumin and 10  $\mu\text{mol/L}$  Fer-1 treatment for 24 hours. (b) Representative cell morphological changes in each group of cells (scale bar = 200  $\mu\text{m}$ ). (c) Effects of Fer-1 on the curcumin-induced accumulation of lipid ROS in A549 and H1299 cells. The level of ROS was detected by fluorescent probe DCFH-DA. (d)–(f) Effects of curcumin and Fer-1 on MDA, SOD, GSH, and iron content in A549 and H1299 cells. (g), (h) Effects of curcumin and Fer-1 on the protein level of ACSL4, SLC7A11, and GPX4. All experiments were done more than three times independently, and all results are expressed as the mean  $\pm$  SD. \* $P < 0.05$ , \*\* $P < 0.002$ , \*\*\* $P < 0.0002$ , \*\*\*\* $P < 0.0001$  versus curcumin group

after being blocked in 5% skim milk for 1 hour at 37°C. The primary antibodies include anti-ACSL4 (1:500), anti-SLC7A11 (1:2000), anti-GPX4 (1:500), anti-IREB2 (1:1000), anti-Beclin1 (1:1000), anti-LC3 (1:1000), anti-P62 (1:1000), and anti- $\beta$ -actin (1:5000). The membrane was incubated with goat anti-rabbit/mouse IgG, HRP-linked antibody (1:5000; CST) for 2 hours at room temperature. Chemiluminescence was performed to visualize all bands.

## Statistical analysis

All data were expressed as mean  $\pm$  standard deviation (SD). Student's *t*-test was used to compare the differences between the two groups. One-way analysis of variance was used to analyze differences among three or more groups. Statistical analysis was performed using the SPSS 20.0 statistical package and GraphPad Prism 7.0 Software.

For all the statistical analyses, a *P*-value  $< 0.05$  was considered statistically significant.

## RESULTS

### Curcumin inhibits tumor growth and promotes cells death in vivo

To validate the antitumor efficacy of curcumin in vivo, we used curcumin to treat LLC-bearing mice and monitored tumor growth for 15 days. The body weight between the vehicle control group and curcumin-treated group was no statistically significant difference. Tumor volume in curcumin group was lower than that of control group (Fig 1a). We investigated the influence of curcumin on cell proliferation and cell death using Ki67 immunofluorescence and H&E staining of tumor sections. As a result, curcumin treatment significantly suppressed

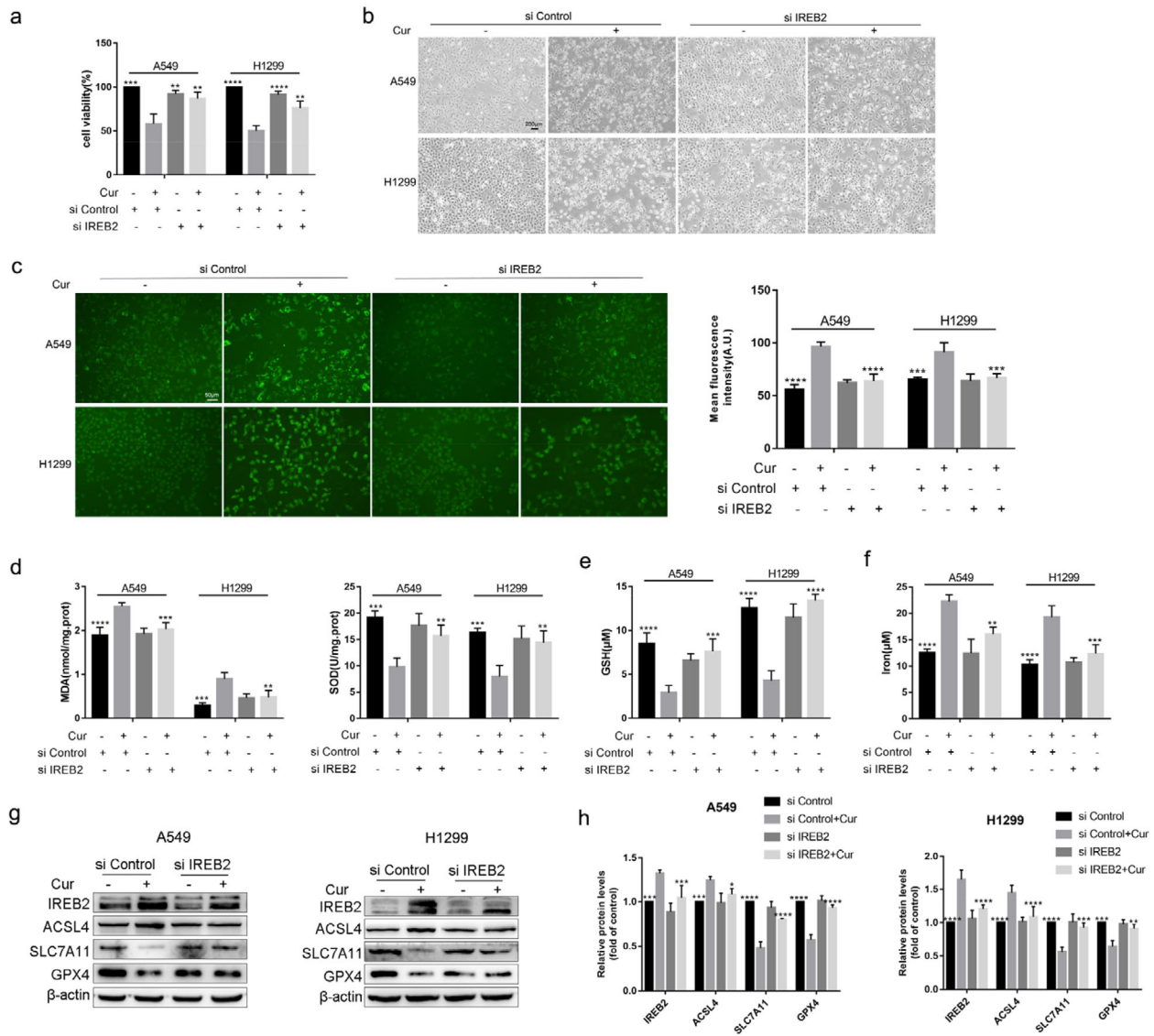


**FIGURE 6** The low expression of IREB2 weakened the sensitivity of A549 and H1299 cells to ferroptosis. (a) The viability of A549 and H1299 cells in siControl group, siControl+curcumin group, siIREB2 group, and siIREB2 + curcumin group. (b) Representative cell morphological changes in each group of cells (scale bar = 200  $\mu$ m). (c)–(f) The contents of ROS, MDA, SOD, GSH, and iron in each group of cells. (g) The protein expression of IREB2, ACSL4, SLC7A11, and GPX4 in each group of cells. (h) Semi-quantitative analysis of immunoblotting results. All experiments were done more than three times independently, and all results are expressed as the mean  $\pm$  SD. \* $P$  < 0.05, \*\* $P$  < 0.002, \*\*\* $P$  < 0.0002, \*\*\*\* $P$  < 0.0001 versus siControl+curcumin group

the proliferation of tumor cells (Fig 1b) and promoted the death of tumor cells (Fig 1c).

### Curcumin suppresses cell proliferation and promotes cell death in vitro

To estimate the cytotoxicity for the A549 and H1299 cells caused by curcumin, we treated growing cells with curcumin at different concentrations and different times. CCK-8 assays showed that curcumin reduced cell viability in a dose- and time-dependent manner (Fig 2a). We further examined the effect of curcumin on cell proliferation using Ki67 immunofluorescence, and we found that curcumin inhibited cell proliferation (Fig 2b,c). To evaluate the effect

of curcumin on cell death, cell morphology was observed. The results suggested curcumin greatly increased the number of dead cells (Fig 2d).

### Curcumin induces characteristic changes of ferroptosis in mice

It is well known that lipid peroxidation, GSH depletion, and the accumulation of iron are critical events in ferroptosis.<sup>12</sup> To explore whether curcumin induced ferroptosis in vivo, we first detected levels of MDA, SOD, GSH, and iron in tumor tissue. Compared with the control group, MDA contents were significantly higher, and SOD activity was significantly lower in the curcumin-treated group (Fig 3a).

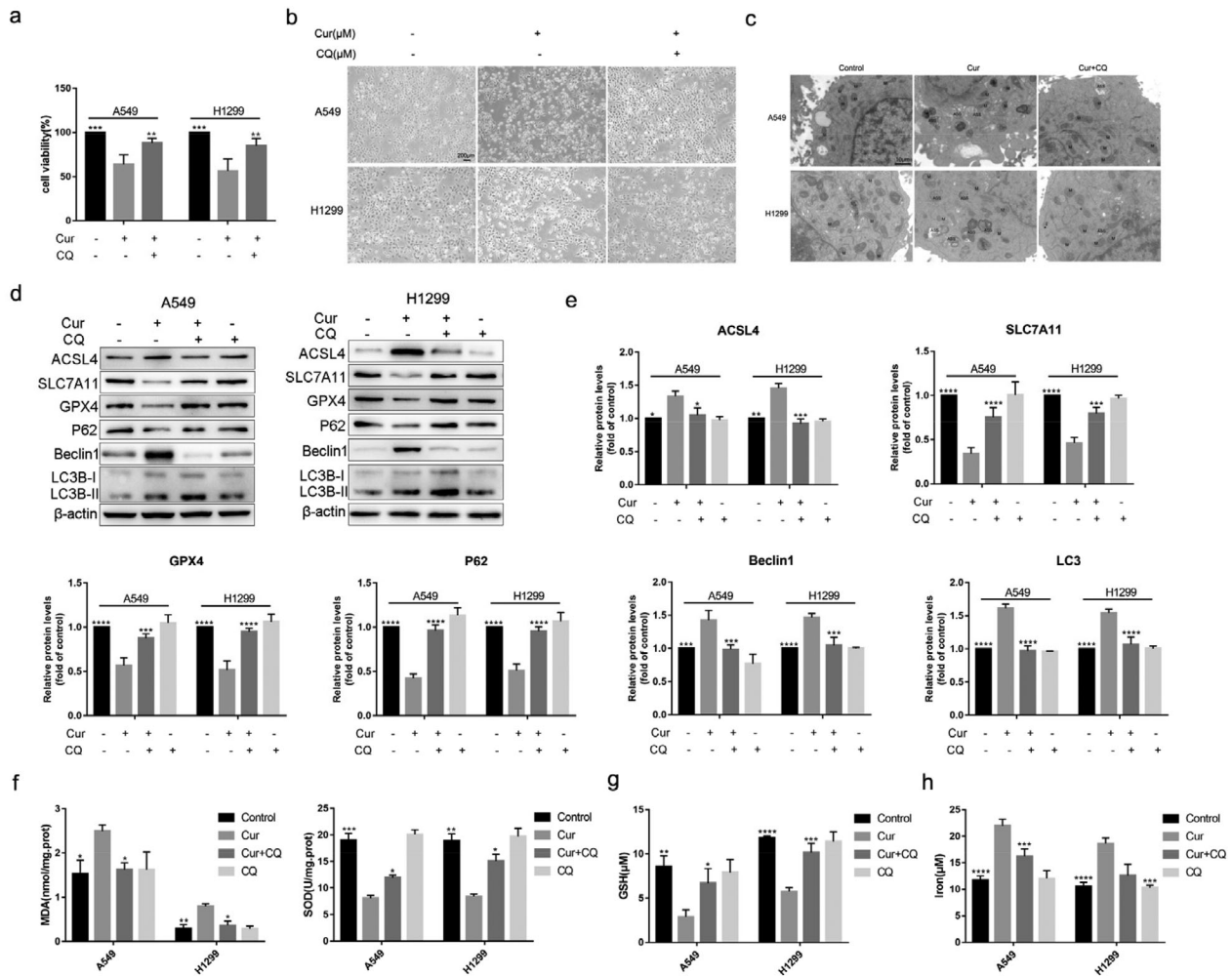


**FIGURE 7** Curcumin-induced cellular ferroptosis was alleviated by CQ. (a) Cell viability was measured after 30  $\mu\text{mol/L}$  curcumin and 20  $\mu\text{mol/L}$  CQ treatment for 24 hours. (b) Representative cell morphological changes in each group of cells (scale bar = 200  $\mu\text{m}$ ). (c) Effects of curcumin and CQ on autolysosome and ultrastructural features of mitochondrion in A549 and H1299 cells (scale bar = 10  $\mu\text{m}$ ). (d) The effect of CQ on protein levels of P62, Beclin1, LC3, ACSL4, SLC7A11, and GPX4 in curcumin-treated A549 and H1299 cells. (e) Semi-quantitative analysis of immunoblotting results. (f)–(h) Effects of curcumin and CQ on MDA, SOD, GSH, and iron content in A549 and H1299 cells. All results are expressed as the mean  $\pm$  SD. \* $P < 0.05$ , \*\* $P < 0.002$ , \*\*\* $P < 0.0002$ , \*\*\*\* $P < 0.0001$  versus curcumin group

Meanwhile, curcumin increased GSH depletion (Fig 3b) and the content of iron in tumor tissue (Fig 3c). We then detected biomarker of ferroptosis. Western blotting results showed that the protein level of ACSL4 in the tumor tissue of mice was obviously upregulated, and the level of SLC7A11 and GPX4 was significantly downregulated by curcumin (Fig 3d). The immunohistochemical analysis also indicated that the protein level of ACSL4 was higher and the level of GPX4 was lower in the curcumin group than that in the control group (Fig 3e). Therefore, we suggested that curcumin could induce ferroptosis in vivo.

### Curcumin triggers ferroptosis in A549 and H1299 cells

For further confirmation, the A549 and H1299 cells were treated with different concentrations of curcumin. The results showed

that a distinct dose-dependent change of MDA, SOD, GSH, and iron contents (Fig 4a–c) and the protein levels of ACSL4, SLC7A11, and GPX4 (Fig 4d,e) occurred after curcumin treatment compared with the control group. In brief, all data showed that curcumin triggered ferroptosis in A549 and H1299 cells.

### Inhibition of ferroptosis by Fer-1 mitigated the sensitivity of A549 and H1299 cells to cell death induced by curcumin

Fer-1, a specific inhibitor of ferroptosis, was used to further explore whether ferroptosis was involved in antitumor effect of curcumin. We found that the cell viability (Fig 5a) was significantly higher, and the number of dead cells (Fig 5b) was lower in curcumin+fer-1 group than that in curcumin group. Additionally, after being pretreated with Fer-1, ROS, and MDA, contents were apparently reduced, and the

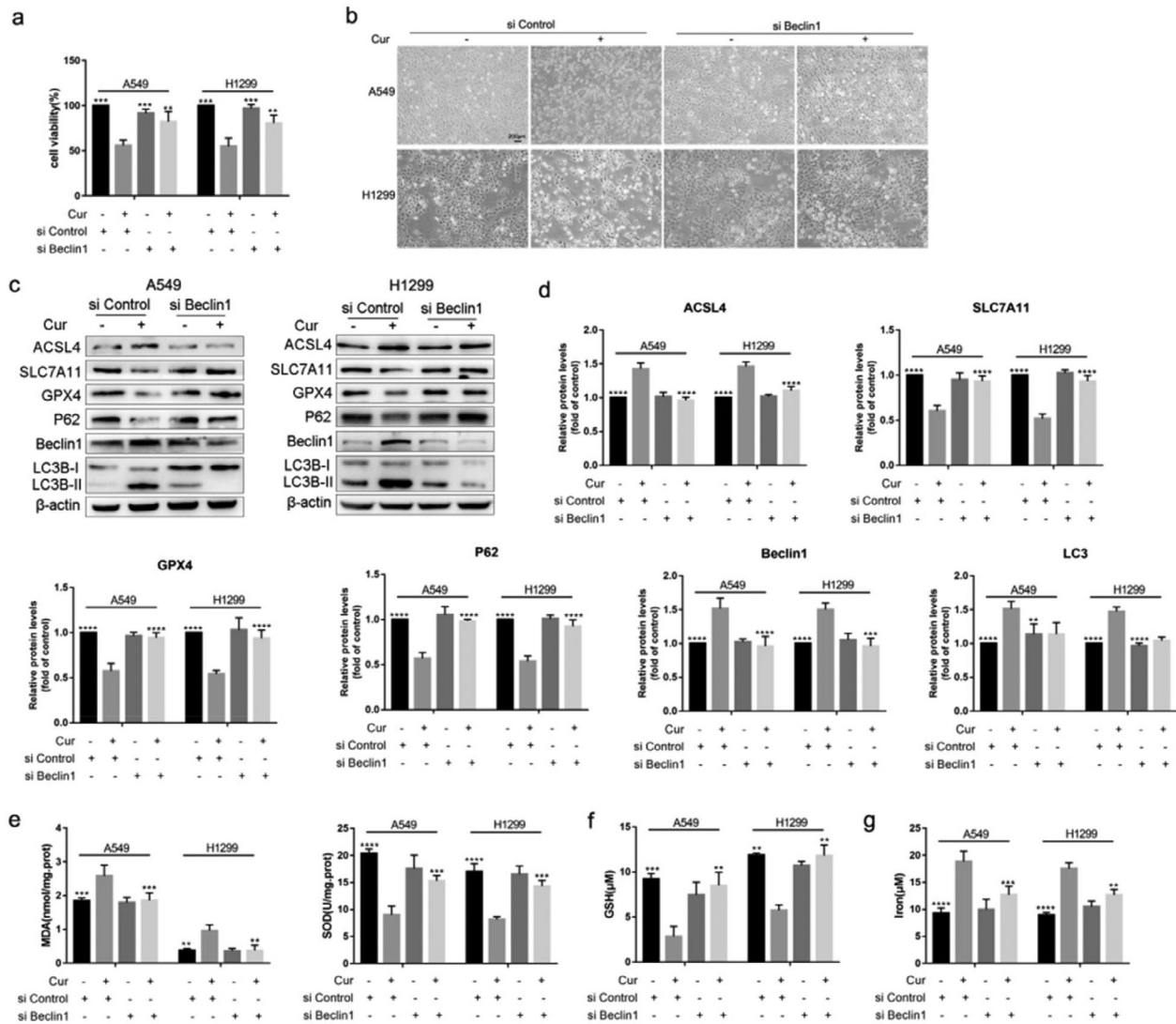


**FIGURE 8** Knockdown Beclin1 reverses ferroptosis related indicators in A549 and H1299 cells. (a) The viability of A549 and H1299 cells in siControl group, siControl+curcumin group, siBeclin1 group, and siBeclin1+curcumin group. (b) Representative cell morphological changes in each group of cells (scale bar = 200  $\mu$ m). (c) The protein expression levels of P62, Beclin1, LC3, ACSL4, SLC7A11 and GPX4 in each group of cells. (d) Semi-quantitative analysis of immunoblotting results. (e)–(g) The concentrations of MDA, SOD, GSH, and iron in each group of cells. All results are expressed as the mean  $\pm$  SD. \*\* $P$  < 0.002, \*\*\* $P$  < 0.0002, \*\*\*\* $P$  < 0.0001 vs. siControl+curcumin group

activity of SOD and GSH were greatly increased (Fig 5c–e). Meanwhile, Fer-1 rescued the cumulation of iron induced by curcumin (Fig 5f). Fer-1 reduced ACSL4 protein expression and increased the protein level of SLC7A11 and GPX4 (Fig 5g,h). In general, these results indicated that Fer-1 inhibited cell death and characteristic changes of ferroptosis in curcumin-treated A549 and H1299 cells.

### Silence of IREB2 alleviated the sensitivity of A549 and H1299 cells to ferroptosis

SiIREB2 was transfected into A549 and H1299 cells to down-regulate the expression level of IREB2. Similar to the effects of Fer-1, siIREB2 transfection obviously alleviated the effects of curcumin on inhibited cell viability and increased cell death

(Fig 6a,b). Meanwhile, compared with siControl+curcumin group, the contents of ROS, MDA, and iron were decreased, and the level of SOD and GSH were increased in siIREB2+curcumin group (Fig 6c–f). Furthermore, the protein expression levels of IREB2 and ACSL4 was lower, and the expression of SLC7A11 and GPX4 were higher in siIREB2+curcumin group than that in siControl+curcumin group (Fig 6g,h). These results suggest that ferroptosis might participate in anti-NCSLC effects of curcumin.

### Inhibition of autophagy attenuated curcumin-induced ferroptosis in A549 and H1299 cells

Studies have shown that autophagy increases ferroptosis by ferritin and transferrin receptor regulation.<sup>5,13</sup> However,

whether ferroptosis induced by curcumin in NSCLC is associated with autophagy is unclear. Therefore, we first observed whether autophagy was triggered by curcumin in A549 and H1299 cells. As shown in Figures 7 and 8, compared with the control group, autolysosome was accumulated, the biomarker of autophagy Beclin1 and LC3 was increased, and P62 was decreased in the curcumin group.

We downregulated basal autophagy using CQ (an inhibitor of autophagosome-lysosome fusion) or silencing the autophagy-related gene Beclin1 (siBeclin1) in the A549 and H1299 cells. The results showed that cell viability was increased and the number of dead cells was decreased after CQ pretreatment or siBeclin1 interference (Figs 7a,b and 8a,b). Additionally, the increased autophagy caused by curcumin was reversed by CQ or siBeclin1 (Figs 7c–e and 8c,d). Subsequently, we found that curcumin-induced mitochondrial membrane rupture and cristae reduction were rescued by CQ (Fig 7c). And western blotting results also showed that the increased expression of ACSL4 and decreased GPX4, SLC7A11 were overturned by CQ or siBeclin1 in curcumin group (Figs 7d,e and 8c,d). Furthermore, after pretreatment with CQ or siBeclin1, overloaded MDA and iron and impaired SOD and GSH caused by curcumin were alleviated (Figs 7f–h and 8e–g). In conclusion, the results suggest that autophagy contributed to curcumin-induced ferroptosis of NSCLC, and blocking autophagy alleviated the sensitivity of cells to cellular ferroptosis.

## DISCUSSION

Cell death has a significant part to play in preventing and treating hyperproliferative diseases such as cancer.<sup>14</sup> Ferroptosis, a novel form of cell death, is distinct from necrosis, apoptosis, and autophagy in terms of morphology, biochemistry, and genetics.<sup>15,16</sup> Emerging studies have shown that ferroptosis is crucial in regulating growth of tumors, such as NSCLC, glioblastoma, renal cell carcinoma (RCC), and hepatocellular carcinoma (HCC).<sup>17,18</sup> Therefore, ferroptosis pathway may open up a new way for the use of anticancer drugs.

Previous researches have suggested that curcumin could suppress tumor growth via inhibiting cell proliferation, inducing apoptosis and activating autophagy, and present low side effects and toxicity.<sup>19</sup> However, the role of curcumin in ferroptosis is not well understood. Guerrero-Hue *et al.* found that curcumin could prevent renal injury by reducing ferroptotic cell death.<sup>20</sup> Whereas Chen *et al.* showed that ferroptosis were observed in glioblastoma cell after treatment of curcumin analog.<sup>9</sup> Li *et al.* found that curcumin triggers ferroptosis in breast cancer cells.<sup>10</sup>

In this research, we observed whether ferroptosis occurred in NSCLC cells under curcumin treatment both in vitro and in vivo. These data suggested that curcumin significantly triggered the cytological and molecular characteristics of ferroptotic cell death in LLC-bearing mice, A549,

and H1299 cells, including the depletion of GSH, lipid peroxidation, and the accumulation of ROS and iron. In addition, the ferroptosis inhibitor Fer-1 pretreatment or siIREB2 interference could reduce curcumin-induced ferroptosis in A549 and H1299 cells. All data indicated that curcumin can promote ferroptosis, which is beneficial to the treatment of NSCLC.

As a self-degradation system, autophagy is a double-edged sword, which could suppress tumor initiation but accelerate tumor progression.<sup>21</sup> There is growing evidence that the autophagy machinery plays an essential role in ferroptosis,<sup>22</sup> and excessive autophagy can promote ferroptosis through the accumulation of iron or lipid peroxidation.<sup>23</sup> Our data demonstrated that pretreatment with CQ or knockout of autophagy-related genes Beclin1 could reduce curcumin-induced autophagy and following ferroptosis in A549 and H1299 cells, indicating that the activation of autophagy pathway can trigger ferroptosis of tumor cells. This may be due to the fact that the up-regulated autophagy could degrade ferritin, regulate the intracellular iron homeostasis, promote the production of ROS, and then lead to ferroptosis.<sup>24</sup> Autophagy can provide free iron for ferroptosis through nuclear receptor coactivator-mediated ferritinophagy.<sup>25</sup>

Limitations still exist in this study. First, the potential mechanisms of autophagy promoting ferroptosis in NSCLC-suppressive effect of curcumin have not been explored. Second, animal models are needed to provide more evidence for research results. Third, activity of curcumin in vivo is limited because of its low bioavailability, poor water solubility, and fast metabolism.<sup>26</sup> To solve this problem, researchers are trying to explore new drug delivery systems, such as liposomes, solid dispersions, and microemulsions.<sup>3</sup>

In conclusion, our results provide evidence that curcumin could induce ferroptotic cell death of NSCLC cells via activating autophagy. All these findings suggest that ferroptosis has the important potential of being a novel approach in anti-NSCLC therapies. Consequently, the combination of ferroptosis-inducing drugs and other anti-cancer methods can be prospectively used to improve the effects of anti-tumor treatments.

## ACKNOWLEDGMENTS

This study was supported by grants from the National Natural Science Foundation of China (No. 81670084, 81970084), National key research and development program of China (No. 2016YFC1304502) and the Tianjin Key Research and Development Program (No. 20YFZCSY00390).

## CONFLICTS OF INTEREST

The author reports no conflicts of interest in this work.

## ORCID

Xin Tang  <https://orcid.org/0000-0002-0372-478X>

Maoli Liang  <https://orcid.org/0000-0002-5112-0892>

Qianqian Chen  <https://orcid.org/0000-0002-2879-0310>

Jie Cao  <https://orcid.org/0000-0001-6058-4608>

## REFERENCES

1. Bray F, Ferlay J, Soerjomataram I, Siegel RL, Torre LA, Jemal A. Global cancer statistics 2018: GLOBOCAN estimates of incidence and mortality worldwide for 36 cancers in 185 countries. *CA Cancer J Clin*. 2018;68:394–424.
2. Rosas G, Ruiz R, Araujo JM, Pinto JA, Mas L. ALK rearrangements: Biology, detection and opportunities of therapy in non-small cell lung cancer. *Crit Rev Oncol Hematol*. 2019;136:48–55.
3. Feng T, Wei Y, Lee RJ, Zhao L. Liposomal curcumin and its application in cancer. *Int J Nanomedicine*. 2017;12:6027–44.
4. Hirsch FR, Scagliotti GV, Mulshine JL, Kwon R, Curran WJ Jr, Wu YL, et al. Lung cancer: Current therapies and new targeted treatments. *Lancet*. 2017;389:299–311.
5. Hou W, Xie Y, Song X, Sun X, Lotze MT, Zeh HJ III, et al. Autophagy promotes ferroptosis by degradation of ferritin. *Autophagy*. 2016;12:1425–8.
6. Yilong Z, Michael JP, Amy AD, Li H, Eaton JK, Wang W, et al. A GPX4-dependent cancer cell state underlies the clear-cell morphology and confers sensitivity to ferroptosis. *Nat Commun*. 2019;10:1617.
7. Torii S, Shintoku R, Kubota C, Yaegashi M, Torii R, Sasaki M, et al. An essential role for functional lysosomes in ferroptosis of cancer cells. *Biochem J*. 2016;473:769–77.
8. Tomeh MA, Hadianamrei R, Zhao X. A review of curcumin and its derivatives as anticancer agents. *Int J Mol Sci*. 2019;20:1033.
9. Chen TC, Chuang JY, Ko CY, Kao TJ, Yang PY, Yu CH, et al. AR ubiquitination induced by the curcumin analog suppresses growth of temozolomide-resistant glioblastoma through disrupting GPX4-mediated redox homeostasis. *Redox Biol*. 2020;30:101413.
10. Li R, Zhang J, Zhou Y, Gao Q, Wang R, Fu Y, et al. Transcriptome investigation and in vitro verification of curcumin-induced HO-1 as a feature of ferroptosis in breast cancer cells. *Oxid Med Cell Longev*. 2020;2020:3469840.
11. Park E, Chung SW. ROS-mediated autophagy increases intracellular iron levels and ferroptosis by ferritin and transferrin receptor regulation. *Cell Death Dis*. 2019;10:822.
12. Stockwell BR, Friedmann AJP, Bayir H, Bush AI, Conrad M, Dixon SJ, et al. Ferroptosis: A regulated cell death nexus linking metabolism, redox biology, and disease. *Cell*. 2017;171:273–85.
13. Wei S, Qiu T, Yao X, Wang N, Jiang L, Jia X, et al. Arsenic induces pancreatic dysfunction and ferroptosis via mitochondrial ROS-autophagy-lysosomal pathway. *J Hazard Mater*. 2020;384:121390.
14. Guo J, Xu B, Han Q, Zhou H, Xia Y, Gong C, et al. Ferroptosis: A novel anti-tumor action for Cisplatin. *Cancer Res Treat*. 2018;50:445–60.
15. Yagoda N, von Rechenberg M, Zaganjor E, Bauer AJ, Yang WS, Fridman DJ, et al. RAS-RAF-MEK-dependent oxidative cell death involving voltage-dependent anion channels. *Nature*. 2007;447:864–8.
16. Dixon SJ, Lemberg KM, Lamprecht MR, Skouta R, Zaitsev EM, Gleason CE, et al. Ferroptosis: An iron-dependent form of non-apoptotic cell death. *Cell*. 2012;149:1060–72.
17. Chen P, Wu Q, Feng J, Yan L, Sun Y, Liu S, et al. Erianin, a novel dibenzyl compound in dendrobium extract, inhibits lung cancer cell growth and migration via calcium/calmodulin-dependent ferroptosis. *Signal Transduct Target Ther*. 2020;5:51.
18. Xia X, Fan X, Zhao M, Zhu P. The relationship between Ferroptosis and tumors: A novel landscape for therapeutic approach. *Curr Gene Ther*. 2019;19:117–24.
19. Mehta HJ, Patel V, Sadikot RT. Curcumin and lung cancer—A review. *Target Oncol*. 2014;9:295–310.
20. Guerrero-Hue M, Garcia-Caballero C, Palomino-Antolin A, Rubio-Navarro A, Vázquez-Carballo C, Herencia C, et al. Curcumin reduces renal damage associated with rhabdomyolysis by decreasing ferroptosis-mediated cell death. *FASEB J*. 2019;33:8961–75.
21. Onorati AV, Dyczynski M, Ojha R. Targeting autophagy in cancer. *Cancer-Am Cancer Soc*. 2018;124:3307–18.
22. Kang R, Tang D. Autophagy and Ferroptosis - What's the connection? *Curr Pathobiol Rep*. 2017;5:153–9.
23. Ma S, Henson ES, Chen Y, Gibson SB. Ferroptosis is induced following siramesine and lapatinib treatment of breast cancer cells. *Cell Death Dis*. 2016;7:e2307.
24. Zhou B, Liu J, Kang R, Klionsky DJ, Kroemer G, Tang D. Ferroptosis is a type of autophagy-dependent cell death. *Semin Cancer Biol*. 2020;66:89–100.
25. Latunde-Dada GO. Ferroptosis: Role of lipid peroxidation, iron and ferritinophagy. *Biochim Biophys Acta Gen Subj*. 1861;2017:1893–900.
26. Sharifi S, Fathi N, Memar MY, Hosseiniyan Khatibi SM, Khalilov R, Negahdari R, et al. Anti-microbial activity of curcumin nanoformulations: New trends and future perspectives. *Phytother Res*. 2020;34:1926–46.

**How to cite this article:** Tang X, Ding H, Liang M, et al. Curcumin induces ferroptosis in non-small-cell lung cancer via activating autophagy. *Thorac Cancer*. 2021;12:1219–1230. <https://doi.org/10.1111/1759-7714.13904>